Polym. Bull. (2011) 67:1185–1200
DOI 10.1007/s00289-011-0446-7

ORIGINAL PAPER

"One pot" synthesis of fluorinated block copolymers using a surface-active ATRP initiator under emulsion polymerization conditions

Jinbing Shu · Chuanjie Cheng · Yi Zheng · Liang Shen · Yongluo Qiao · Changqing Fu

Received: 30 August 2010 / Revised: 31 December 2010 / Accepted: 1 January 2011 /
Published online: 22 January 2011

Abstract Three fluorinated block copolymers have been prepared successfully in emulsion system using a surface-active atom transfer radical polymerization (ATRP) initiator disodium 4-(10-(2-bromo-2-methylpropanoyloxy)decyloxy)-4-oxo-2-sulfonatobutanoate (**1**). The copolymerization can be conducted in "one pot" under activator generated by electron transfer (AGET) ATRP in emulsion conditions, thus greatly simplifying the operations and workup. The anionic surface-active ATRP initiator (**1**) and nonionic surfactant OP-10 may form synergistic stabilizers that effectively guarantee stability of the final latex. The ATRP follows first-order kinetics and has living/controlled characteristics based on the researching results of polymerization of trifluoroethyl methacrylate (TFEMA). Surface studies indicate that the fluorinated block copolymers reveal lower surface energy and stronger hydrophobic property compared with those non-fluorinated polymers. The decreasing order of surface energy of the polymers is: polystyrene (PS) > polytrifluoroethyl methacrylate-*block*-polystyrene (PTFEMA-*b*-PS) > polyhexafluorobutyl methacrylate-*block*-polystyrene (PHFBMA-*b*-PS) > polydodecafluoroheptyl methacrylate-*block*-polystyrene (PDFHMA-*b*-PS) > polydodecafluoroheptyl methacrylate (PDFHMA). Fluorinated homopolymer PDFHMA and copolymer PDFHMA-*b*-PS exhibits relatively low-surface energy, which is ascribed to the long and flexible DFHMA units containing in the polymers.

Keywords Surface-active · Fluorinated copolymers · ATRP initiator · AGET ATRP · Emulsion polymerization

J. Shu · C. Cheng (✉) · Y. Zheng · L. Shen (✉) · Y. Qiao · C. Fu
Jiangxi Key Laboratory of Organic Chemistry, Jiangxi Science & Technology Normal University, Fenglin Street, Nanchang 330013, Jiangxi, People's Republic of China
e-mail: chengcj530@gmail.com

L. Shen
e-mail: shenliang00@tsinghua.org.cn

Introduction

Living/controlled radical polymerization (LRP) has attracted much interest due to its great significance in academics and potential applications in industry [1–5]. As one of the most important LRP method, atom transfer radical polymerization (ATRP) has been widely studied because of its advantages such as controllable polymer molecular weight, narrow molecular weight distribution, adaptability to most monomers, designable molecular structures (e.g., comb-like, star-like, telechelic, block and gradient polymers, etc.) [6], and commercially available ATRP initiators [7–11]. Moreover, ATRP approach can tolerate many functional groups [12]; thus, some functionalized molecules have been designed and prepared by this method [13, 14].

ATRP can be conducted in various reaction systems such as bulk, solution, emulsion, and suspension, but the increasing environmental pressure in recent years has prompted chemists to research greener reaction media [9]. For example, some environmentally benign solvents such as supercritical CO_2, ionic liquids, and poly(ethylene glycol) were used in ATRP reactions [15–17]. However, the above reaction media still suffer from high cost compared to common organic solvents, and some properties of ionic liquids such as toxicity and biodegradability are still unclear [18]. Water is a well-known environmentally friendly solvent for many inorganic and organic reactions, therefore, ATRP under water-based emulsion or suspension polymerization conditions has been widely studied and great progress has been made in recent years [19–24].

In common emulsion polymerizations, conventional small molecular emulsifiers must be added to stabilize the reaction system. However, these small molecular emulsifiers will stay in the final polymers, thus causing negative effects on the electrical, optical, surface, water resistance, and film-forming performance of the polymer products. Therefore, reactive emulsifiers, amphiphilic macro-emulsifiers, and emulsifier-free emulsion polymerizations are extensively researched in order to solve the above problems [25]. The strategies have also been applied to the living radical emulsion polymerizations. For instance, Li et al. applied PEO-based nonionic surface-active ATRP macroinitiator to emulsifier-free miniemulsion polymerizations of butyl acrylate (BA) [26]. Stoffelbach et al. have reported a cationic surface-active ATRP initiator which was successfully used in soap-free miniemulsion polymerization of methyl methacrylate (MMA) [27]. Rieger et al. described surfactant-free living/controlled radical emulsion copolymerization of *n*-butyl acrylate and methyl methacrylate via RAFT using amphiphilic poly(ethylene oxide)-based trithiocarbonate chain transfer agents [28]. Wang et al. designed an amphiphilic poly(acrylic acid-*b*-styrene) trithiocarbonate RAFT agent and utilized it in ab initio batch emulsion polymerization of styrene [29]. Similarly, Yan's group prepared a core–shell polymer via an amphiphilic RAFT agent under emulsion polymerization conditions [30]. Very recently, our group has reported the synthesis and application of an anionic surface-active ATRP initiator to activator generated by electron transfer (AGET) ATRP emulsion polymerization of MMA, and stable latex was obtained without any other added emulsifier [24]. AGET ATRP is a

method developed by Matyjaszewski's research group, in which a high-valent metal catalyst (e.g., $CuBr_2$) together with an appropriate reducing agent (e.g., ascorbic acid) can substitute low valent metal catalyst (e.g., CuCl) used in normal ATRP [31–33]. AGET ATRP can effectively overcome the drawback of air sensitivity in ATRP.

Fluorinated polymers have become significant functional materials with low-surface energy, good thermal stability, outstanding chemical resistance, excellent electrical properties, etc. [34, 35]. However, high cost of perfluoro polymers has limited their practical applications, and studies of non-perfluoro polymers have attracted much interest in recent years. Herein, we will extend the application of our anionic surface-active ATRP initiator to the preparation of fluorinated block copolymers. It is well known that copolymers are usually advantageous over their corresponding homopolymers in strength, chemical resistance, low cost, and other performance [36, 37]. Moreover, "one pot" copolymerization of fluorine-containing monomers with styrene was implemented, thus avoiding the tedious procedure in stepwise preparation of block copolymers in literature.

Experiment

Materials

Commercial $CuBr_2$, bis(2-pyridylmethyl)octadecylamine (BPMODA), ascorbic acid (AA), tetrahydrofuran (THF), and neutral Al_2O_3 were all AR grade purity and were used directly as received. All the monomers including styrene (97%), trifluoroethyl methacrylate (TFEMA, 99%), hexafluorobutyl methacrylate (HFBMA, 98%), and dodecafluoroheptyl methacrylate (DFHMA, 98%) were washed in 5% aqueous NaOH and then distilled under reduced pressure to remove the inhibitor prior to use. The anionic surface-active ATRP initiator disodium 4-(10-(2-bromo-2-methylpropanoyloxy)decyloxy)-4-oxo-2-sulfonatobutanoate (**1**) was synthesized according to the literature [24]. Nonionic emulsifier octylphenol polyoxyethylene ether-10 (OP-10) was CP grade and used directly as received.

Characterization

The structures of polymers were characterized by ^{1}H NMR and ^{13}C NMR spectroscopy on a Bruker AV 400 MHz spectrometer, with tetramethylsilane (TMS) as the standard. $CDCl_3$ was used as the solvent. Gel permeation chromatography (GPC) was performed on an HP 1100 HPLC, equipped with a Waters 2414 refractive index detector and three Styragel HR 2, HR 4, HR 5 of 300 × 7.5 mm columns (packed with 5 mm particles of different pore sizes). The column packing allowed the separation of polymers over a wide molecular weight range of 500–1,000,000. THF was used as the eluent at a flow rate of 1 mL min^{-1} at 40 °C. PMMA standards were used as the reference. The FTIR spectra were recorded via the KBr pellet method using a Bruker V70 FTIR spectrophotometer. The average

particle diameter (D_z) and particle size distribution (PSD) were determined on a Rize-2008 laser particle size analyzer. Contact angles and surface energy of the copolymers were measured by a JC2000C1 contact angle meter (Shanghai, China). Scanning electron microscopy (SEM) of the latex was finished on Tescan VEGA-II scanning electron microscope produced by Tescan USA Incorporation.

AGET ATRP of TFEMA in emulsion with initiator **1** as both an initiator and a surfactant

A mixture of $CuBr_2$ (0.023 g, 0.104 mmol), BPMODA (0.047 g, 0.104 mmol), and TFEMA (1 g, 5.95 mmol) was stirred in a flask at room temperature for 15 min to form the Cu(II) complex. During this process, aqueous initiator **1** (0.95 g, 10 wt%, 0.174 mmol) was added dropwise into the complex. Then the above resulting mixture was slowly introduced into an aqueous solution (40 mL) of OP-10 (0.124 g, 0.196 mmol) and initiator **1** (0.75 g, 10 wt%, 0.137 mmol) in a 100-mL three-necked flask under stirring to form a clear microemulsion. The microemulsion was purged with nitrogen for 30 min, and after that the flask was put into an oil bath thermostated at 80 °C. An aqueous solution (5 mL) of ascorbic acid (0.018 g, 0.102 mmol) was injected into the microemulsion to initiate polymerization. Fifteen minutes later, the second part of TFEMA monomer (2.50 g, 14.88 mmol) was added to the microlatex. During polymerization process, samples were withdrawn periodically to measure monomer conversions by gravimetry.

Before gel permeation chromatography (GPC) analysis, the polymer products containing blue Cu^{2+} residue are chromatographed with neutral Al_2O_3 to remove the undesired Cu^{2+}, using THF as the eluant.

Block copolymerization of TFEMA with styrene by AGET ATRP in emulsion using initiator **1** as both an initiator and a surfactant in "one pot"

To the PTFEMA latex prepared in the above procedure, the second kind of monomer styrene (6.45 g, 62.02 mmol) was added. Then the resulting mixture reacted in an oil bath thermostated at 90 °C for hours. Workup of the polymerization is similar to the above experiment.

Copolymers PHFBMA-*b*-PS and PDFHMA-*b*-PS were prepared in a similar manner as that of PTFEMA-*b*-PS.

Measurement of contact angles and surface energy

After purification on an Al_2O_3 column chromatography, the (co)polymers dissolved in THF were spin-coated on a glass substrate to form thin films. Then, water and hexadecane were used to determine contact angles on the (co)polymer surfaces, respectively. The contact angles on the film surfaces were measured by the Sessile drop method, and the experimental data are of the average values obtained from five different points on the film surfaces [38, 39]. Then, surface energy of the (co)polymers was calculated from the contact angle data.

Results and discussion

AGET atom transfer radical emulsion polymerization of TFEMA, PHFBMA, and PDHFMA

We have recently reported the synthesis of the anionic surface-active ATRP initiator **1** and its application in AGET atom transfer radical emulsion polymerization of MMA, where the initiator **1** acted as both an ATRP initiator and an emulsifier (Fig. 1). The polymerization of MMA can be conducted under emulsifier-free conditions with quite stable latex obtained. Yet, when this approach was applied to the polymerization of trifluoroethyl methacrylate (TFEMA) monomer (A01, Table 1), coagulation occurred at the early stage of the reaction and obvious phase separation was observed (Fig. 2a), which may be ascribed to the higher hydrophobic property of TFEMA monomer than that of methyl methacrylate (MMA). Fortunately, when a nonionic surfactant octylphenol polyoxyethylene ether-10 (OP-10) was added to the above polymerization system, stable latex can be obtained (A11–A13, Table 1) (Fig. 2b). This stability may be explained as that the anionic surface-active initiator **1** and the nonionic surface-active OP-10 have synergic interaction to co-stabilize the emulsion system. The deduction was further proved

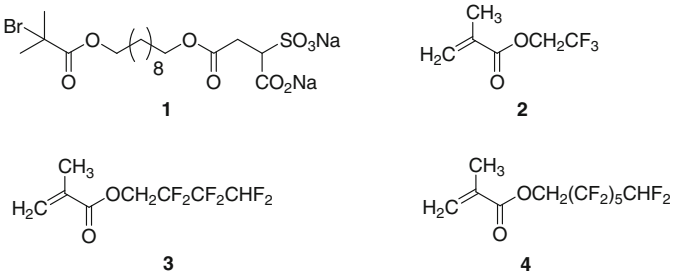

Fig. 1 Structures of the anionic surface-active ATRP initiator (**1**), monomers trifluoroethyl methacrylate monomer (TFEMA) (**2**), hexafluorobutyl methacrylate (HFBMA) (**3**), and dodecafluoroheptyl methacrylate (DFHMA) (**4**)

Table 1 AGET ATRP of TFEMA in emulsion at 80 °C using initiator **1** as both an ATRP initiator and a surfactant and ascorbic acid (AA) as a reducing agent

Exp	TFEMA (wt%)	$[1]_0$[a]	$[EBiB]_0$	$[OP\text{-}10]_0$	$[TFEMA]_0/[1]_0$	$[CuBr_2]_0$	$[AA]_0$
A01	7.02	6.33	0	0	66	1.94	2.02
A02	6.96	0	6.58	4.04	63	2.16	2.00
A11	6.93	6.21	0	3.92	67	2.07	2.05
A12	6.3	6.04	0	3.93	62	1.98	2.11
A13	6.21	5.44	0	4.05	68	2.03	1.99

The molar ratio of ligand BPMODA to $CuBr_2$ was 1:1 for all the experiments, and concentrations are given in mmol L_{latex}^{-1}

[a] Concentration of initiator **1** in the experiments was 10 wt%

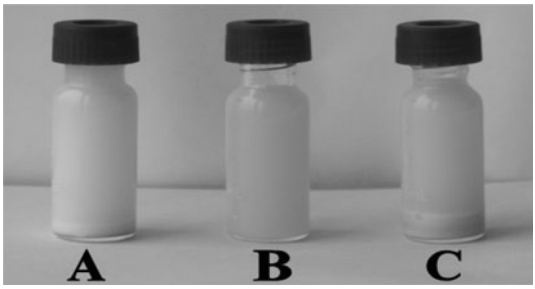

Fig. 2 Appearance of PTFEMA latex from AGET ATRP. **a** Phase separation occurred using only initiator **1** as the surfactant; **b** stable latex was obtained using both initiator **1** and OP-10 as the surfactants; **c** phase separation occurred using only OP-10 as the emulsifier

by the following controlled experiment (A02, Table 1): when ATRP initiator **1** was substituted by a common ATRP initiator ethyl 2-bromoisobutyrate (EBiB) and emulsion polymerization of TFEMA was performed with OP-10 as the only emulsifier, stable latex cannot be formed as shown in Fig. 2c.

Table 2 shows detailed results of the emulsion polymerization of TFEMA, which includes conversion, theoretical number-average molar mass ($M_{n,th}$), the experimental number-average molar mass ($M_{n,GPC}$), and the polydispersity indices (PDI), as well as the average diameters of the latex particles. All the polymerizations of TFEMA (A11–A13, Table 2) proceeded rapidly with high monomer conversions obtained within several hours. When the amount of initiator **1** decreased from 6.21 mmol L_{latex}^{-1} in Exp. A11 to 5.44 mmol L_{latex}^{-1} in Exp. A13, more OP-10 was required to guarantee the latex stability, which suggested that initiator **1** functioned as the stabilizer of the emulsion polymerization. The average diameters determined by laser particle size analyzer are 200–300 nm, indicating that the latex particles have submicrometer size. Furthermore, SEM of PTFEMA latex was shown in Fig. 3 to display morphology and shape of the latex particles, which demonstrated that the latex was composed of uniform sphere-shaped particles with particle size ranging from 200 to 300 nm, and the result was well consistent with that from laser particle size analyzer.

As shown in Fig. 4a, the linear relationship of $\ln([M]_0/[M])$ and the reaction time indicated that the polymerization followed first-order kinetics. The linear fit did not pass the origin point with an intercept on the time axis, indicating a short inhibition period of about 20 min. Figure 4b indicated the dependence of experimental number-average molar mass ($M_{n,exp}$) and polydispersity index (PDI) on TFEMA conversions. Throughout the polymerization reactions, the experimental values of M_n ($M_{n,exp}$) became higher with increasing conversions and were in good agreement with their corresponding theoretical ones, indicating high initiating efficiency of the initiator **1**. Moreover, values of PDI were lower than 1.3 in most polymerizations. Therefore, as stated above, nearly linear relationship of $\ln([M]_0/[M])$ versus reaction time together with relatively low PDI proves the controlled/living features of the emulsion polymerizations.

In addition, Fig. 5 showed the relationship of reaction time and monomer conversions. TFEMA conversions grow almost linearly to a maximal value 88–89% within about 3 h, after which the curve becomes flat even if the concentration of initiator **1** increases from 5.44 to 6.21 mmol L_{latex}^{-1}. Based on this result, in the

Table 2 Characteristics of the PTFEMA latex prepared by AGET ATRP of TFEMA in emulsion with initiator **1** acting as both an ATRP initiator and a latex stabilizer

Exp	Time (min)	Conv. (%)	$M_{n,th}$ (g mol^{-1})	$M_{n,GPC}$[a] (g mol^{-1})	PDI	D_z[b]/nm (PSD)
A11	30	16	1800	2150	1.28	
	50	28	3150	3500	1.29	
	85	47	5290	5950	1.26	
	120	67	7542	7180	1.20	
	160	80	9005	9100	1.21	
	190	89	10018	9760	1.13	
	210	89	10018	10850	1.15	240 (0.18)
A12	35	12	1250	1540	1.26	
	60	23	2396	2820	1.28	
	90	46	4790	4650	1.25	
	125	65	6770	6900	1.27	
	160	83	8645	9280	1.23	
	180	88	9166	9340	1.09	
	210	87	9062	9680	1.15	263 (0.15)
A13	35	13	1485	1520	1.25	
	60	29	3313	3950	1.27	
	90	52	5940	6740	1.32	
	120	69	7883	8260	1.23	
	155	81	9253	9800	1.12	
	180	88	10053	11050	1.09	
	210	88	10053	10700	1.17	289 (0.21)

Theoretical number average molecular weights ($M_{n,th}$) were calculated from the experimentally determined conversions

[a] The experimental number average molecular weights ($M_{n,exp}$) were determined by gel permeable chromatography (GPC) using PMMA standards

[b] Average diameter (D_z) and particle size distribution (PSD) were measured by a laser particle size analyzer

block copolymerization process, TFEMA as the first monomer was polymerized for 3 h with 89% conversion, then, the second monomer styrene can be directly added to the reaction system for further block polymerization.

The other two macroinitiators PHFBMA-Br and PDHFMA-Br were also prepared by AGET ATRP in emulsion in a similar way as that of PTFEMA-Br. Both homopolymerization of HFBMA and that of DHFMA gave living/controlled characteristics according to the kinetic studies, i.e., expected molecular weights and low PDI were obtained (for PHFBMA-Br, $M_{n,GPC} = 11950$, $M_{n,th} = 11260$, PDI = 1.16; for PDHFMA-Br, $M_{n,GPC} = 19950$, $M_{n,th} = 16720$, PDI = 1.21).

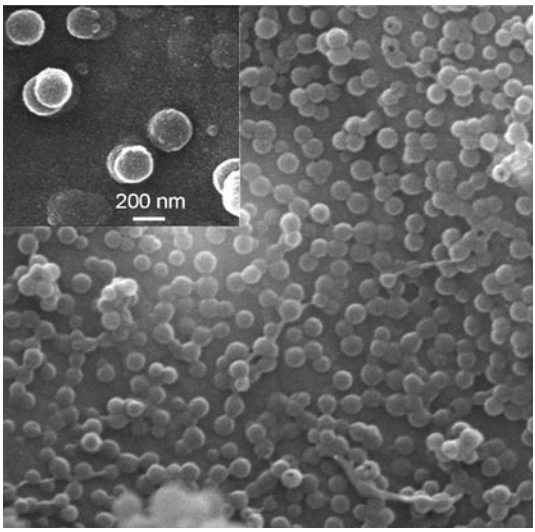

Fig. 3 Scanning electron microscopy (SEM) of the latex of PTFEMA

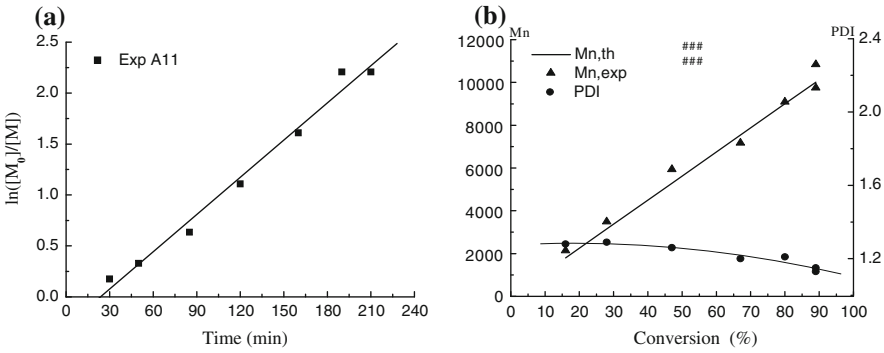

Fig. 4 **a** Experiment A11: dependence of $\ln([M_0]/[M])$ on the reaction time (min), where $[M_0]$ is the initial concentration of the monomer TFEMA and $[M]$ is the concentration of TFEMA at a certain reaction time. **b** Experiment A11: dependence of experimental number-average molecular weight ($M_{n,exp}$) and polydispersity index (PDI) on TFEMA conversions

Fig. 5 Kinetics for the emulsion polymerization of TFEMA at three different concentrations of initiator **1** (Exp A11, $[I]_0 = 6.21$ mmol L^{-1}; Exp A12, $[I]_0 = 6.04$ mmol L^{-1}; Exp A13, $[I]_0 = 5.44$ mmol L^{-1})

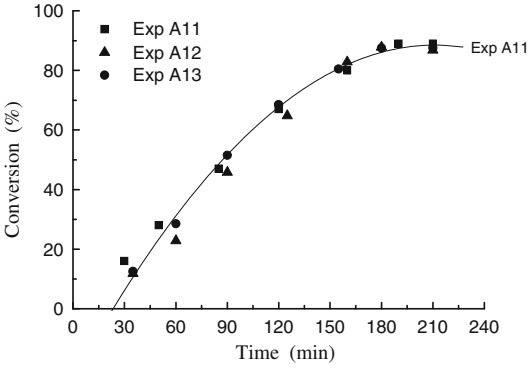

Block copolymerization of TFEMA and styrene by AGET ATRP in emulsion using initiator **1** as both an initiator and a surfactant in "one pot"

AGET ATRP is an efficient technique for synthesis of pure block copolymers, compared with others living radical polymerization methods [40]. Fluorinated polymers are of great significance for their low-surface energy, excellent hydrophobicity and oleophobicity, good weatherability and chemical resistance [41]. However, perfluoro polymers have some disadvantages such as high cost, easy deformation, and low rigidity and hardness. Therefore, it is important to prepare fluorinated copolymers to overcome the above drawbacks [36, 37, 42]. Here, we have prepared PTFEMA-*b*-PS block copolymer using **1** as both an initiator and an emulsifier under AGET ATRP in emulsion conditions (Scheme 1). Firstly, PTFEMA was synthesized as discussed previously. Secondly, styrene as the second monomer was added directly to the PTFEMA latex to start copolymerization, where macroinitiator PTFEMA-Br acted as both a stabilizer and an initiator. After 200 min, conversion of styrene was 72%. Then theoretical molecular weight of the copolymer was calculated as follows:

$$M_{n,th} = \mathrm{Conv}_{styrene} \times M_{n,styrene} \times \left([\mathrm{styrene}]_0/[I]_0\right) + M_{n,PTFEMA} = 72\% \times 104 \times (268/6.21) + 10850 = 14070,$$

where $\mathrm{Conv}_{styrene}$ refers to the conversion of styrene monomer; $M_{n,Styrene}$ and $M_{n,PTFEMA}$ mean the number-average molecular weight of styrene and macroinitiator PTFEMA-Br (Exp. A11, Table 2), respectively; $[\mathrm{styrene}]_0$ and $[I]_0$ refer to the initial concentration of styrene monomer and initiator **1**, respectively.

Kinetic studies for the copolymerization of styrene based on macroinitiator PTFEMA-Br (Exp. A11, Table 2) were also conducted. As shown in Table 3, 32% conversion of styrene can be obtained within 60 min, indicating that the macroinitiator PTFEMA-Br still had high initiating ability. The molecular weight of PTFEMA-*b*-PS increased with the increasing styrene conversion, and the experimental molecular weight ($M_{n,exp}$) was consistent with their corresponding theoretical ones. During the copolymerization of styrene, the data of PDI were about 1.2. Thus, the copolymerization process still featured living characteristics. The increase of chain length was also verified by GPC curves shown in Fig. 6. The GPC

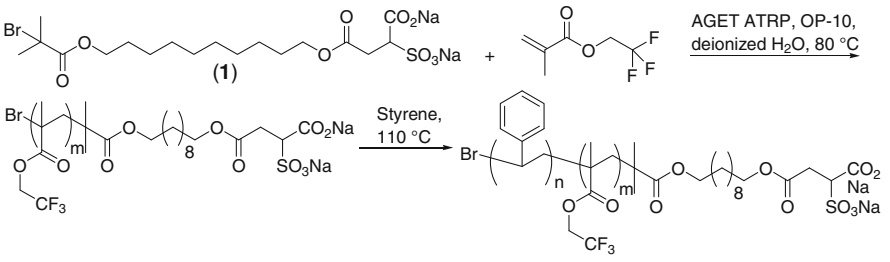

Scheme 1 Preparation of PTFEMA-*b*-PS block copolymer using **1** as both an initiator and an emulsifier under AGET ATRP in emulsion conditions

Table 3 Characteristics of the PTFEMA-*b*-PS copolymer latex prepared using PTFEMA-Br as a macroinitiator

Exp	Time (min)	Conv. (%)	$M_{n,th}$ (g mol^{-1})	$M_{n,GPC}$ (g mol^{-1})	PDI	D_z (nm) (PSD)
A21	0	0	10018	10850	1.15	240
	60	32.4	12308	12920	1.20	
	100	63.6	13705	13430	1.20	
	120	72.1	14070	13650	1.18	
	150	72.8	14116	13590	1.19	346 (0.27)

The macroinitiator was prepared according to experiment A11

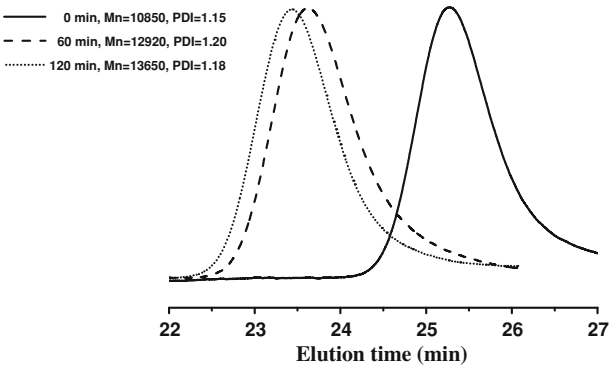

Fig. 6 Comparison of GPC curves of PTFEMA and PTFEMA-*b*-PS

curves of the copolymers obviously shifted to higher molecular weights with extending reaction time while keeping low PDI.

After copolymerization of styrene, the average latex particle size became 346 nm, a little higher than the homopolymer PTFEMA latex. This result may be explained as follows: when the homopolymerization of TFEMA in emulsion was over, the second monomer styrene was added directly to initiate copolymerization in the previously formed latex particles, and no new latex particles formed during the copolymerization of styrene. Therefore, the copolymerization contributed to the increase of both copolymer molecular weights and particle sizes. Figure 7 demonstrated particles sizes and morphology of the copolymer PTFEMA-*b*-PS. The average particle diameter was around 300 nm, but particle size distribution (PSD) of the copolymer PTFEMA-*b*-PS was a little wider than that of PTFEMA. The copolymer particles were roughly spherical shape, but their surface was not so smooth as that of PTFEMA.

To further prove the block structure of the copolymer, ^{1}H NMR spectrum was conducted (Fig. 8). Protons of PTFEMA-*b*-PS were designated as H_a, H_b, etc., as illustrated in Fig. 8. H_a is a unique α-proton of benzyl bromide at the end of the polymer chain, and its chemical shift is at 4.90 ppm. As the number of H_a is one, the

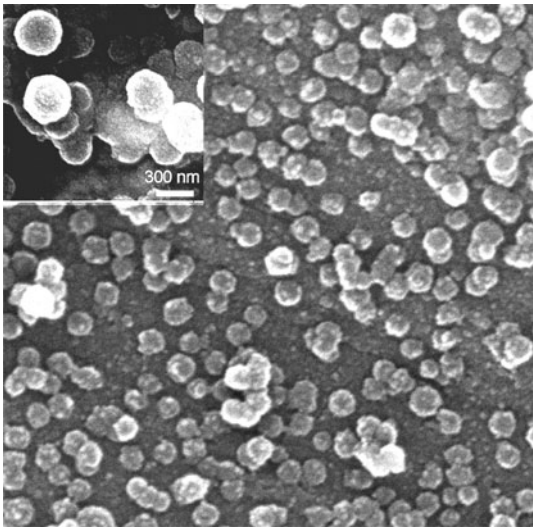

Fig. 7 Scanning electron microscopy (SEM) of the PTFEMA-*b*-PS latex

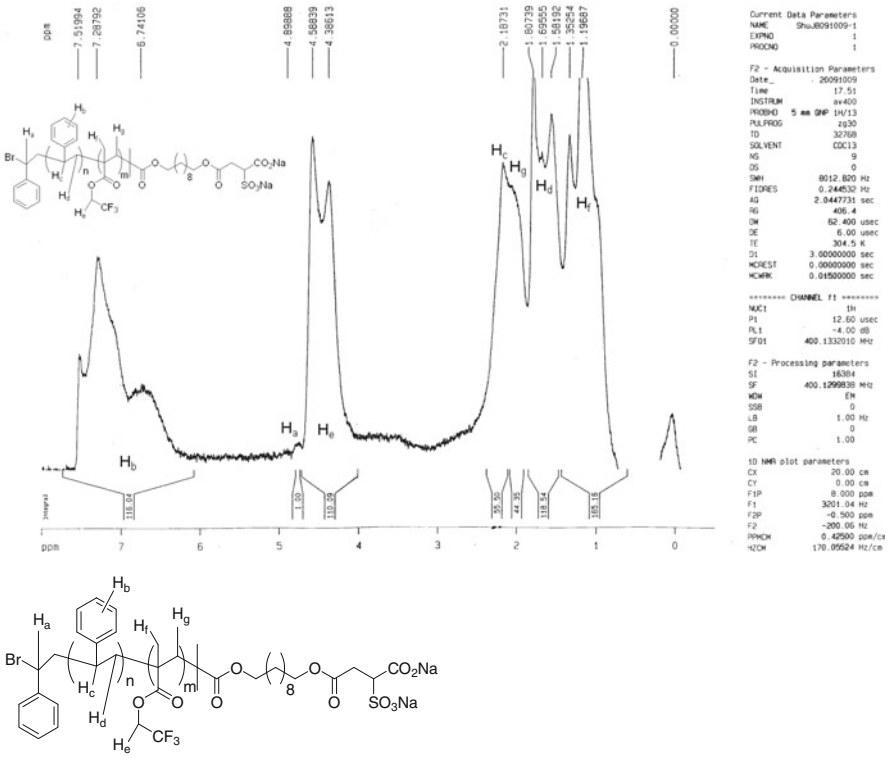

Fig. 8 Structure and ^{1}H NMR spectrum of polytrifluoroethyl methacrylate *block* polystyrene copolymer (PTFEMA-*b*-PS)

integral value of the peak at 4.90 ppm is designated as "1," which is the base of other integral values. The number of H_b that represents protons of phenyl rings is about 115, therefore, the number of phenyl rings is 115 divided by 5, i.e., $n = 23$. Thus, there are totally 23 styrene units in the copolymer chain. H_e is the protons of trifluoroethyl group that is located at about 4.59 ppm in ^{1}H NMR spectrum. The number of H_e is 110, meaning that 55 of TFEMA units exist in the copolymer, i.e., $m = 55$. H_c, H_d, H_f, and H_g are other protons of styrene and TFEMA units. Thus, the number-average molecular weight can be calculated as follows:

$$\begin{aligned} M_{n,NMR} &= m \times M_{n,TFEMA} + n \times M_{n,styrene} + M_I \\ &= 55 \times 168.1 + 23 \times 104.2 + 547 = 12190, \end{aligned}$$

where $M_{n,NMR}$ means the number-average molecular weight of the copolymer, $M_{n,TFEMA}$ is that of TFEMA monomer, and $M_{n,styrene}$ is that of styrene monomer, M_I represents the molecular weight of initiator **1**. The value of $M_{n,NMR}$ (12190) is consistent with that of $M_{n,th}$ (14070) and $M_{n,GPC}$ (13650).

In a similar manner, block copolymers PHFBMA-*b*-PS and PDFHMA-*b*-PS were prepared from their corresponding macroinitiators PHFBMA-Br and PDFHMA-Br, respectively.

Surface properties of copolymers PTFEMA-*b*-PS, PHFBMA-*b*-PS, and PDFHMA-*b*-PS

Surface-free energy is one of the important surface properties of materials. Fluorinated polymers are attractive functional materials with low-surface energy. It is difficult to measure solid surface energy directly, yet it can be calculated from data of contact angles with standard liquids such as polar water and nonpolar hexadecane. Therefore, we have determined contact angles of the prepared fluorinated polymers and copolymers with water and hexadecane, respectively. As shown in Table 4, the three prepared fluorinated copolymers have lower surface energy than non-fluorinated polymers polystyrene (PS), polyethylmethacrylate (PEMA), and polyhexylmethacrylate (PHMA), while they have a little higher surface energy than their corresponding pure fluorinated polymers PTFEM, PHFBMA, and PDFHMA. This result is consistent with our common sense that fluorinated polymers always have lower surface energy than their corresponding non-fluorinated polymers. In comparison with the three fluorinated copolymers, PDFHMA-*b*-PS has the lowest surface energy and the lowest molar percentage of fluorinated units, while PTFEMA-*b*-PS has the highest surface energy and the highest molar percentage of fluorinated units. This indicates that a monomer-like DFHMA with a long fluorine-containing chain plays an important role in lowering surface energy of the corresponding polymer. The phenomenon may be explained as follows: fluorine element has very high electro-negativity compared with carbon and hydrogen elements, and fluorine atoms will bear high-negative charge in C–F single bonds of the molecules. Thus, adjacent fluorine atoms with the same negative charge in molecules have strong repulsive forces, which make chains of macromolecules adopt helical form. This helical form contributes greatly to water

Table 4 Comparison of surface properties of different polymers

Entry	Polymer	Fluorinated units (mol%)[a]	Contact angle with water (°)[b]	Contact angle with hexadecane (°)[b]	Surface energy (mN m^{-1})[c]
1	PTFEMA-*b*-PS	29.2	91.7	45.5	24.1
2	PHFBMA-*b*-PS	20.0	97.5	56.0	19.7
3	PDFHMA-*b*-PS	14.5	104.0	61.5	16.8
4	PS	0	–	–	40.7
5	PEMA	0	–	–	35.9
6	PHMA	0	–	–	30.0
7	PTFEMA	100	93.3	61.2	20.3
8	PHFBMA	100	98.7	66.7	17.2
9	PDFHMA	100	105.3	74.3	13.6

PS polystyrene, *PEMA* polyethylmethacrylate, *PHMA* polyhexylmethacrylate

[a] The molar percentage of fluorinated units in the whole macromolecules

[b] Contact angles were determined at 25 °C

[c] Surface energy values of PTFEMA-*b*-PS, PHFBMA-*b*-PS, and PDFHMA-*b*-PS were calculated from the measured contact angles with water and hexadecane. And the surface energy data of PS, PEMA, and PHMA were obtained from internet: http://www.surface-tension.de/solid-surface-energy.htm

Table 5 Water absorption of different polymers

Polymer	PEMA	PTFEMA	PHFBMA	PDFHMA
Water absorption (%)	28.1	12.9	10.5	8.6

Water absorption $= [(W - W_0)/W_0] \times 100\%$, where W_0 is initial weight of a polymer before absorption of water and W is the weight of the polymer after absorption of water

and oil repellency of fluorinated polymers. Monomers with longer chain are more flexible and easier to form the desired helical form.

Hydrophobicity of polymers can also be tested by water absorption. The less the water absorption is, the more hydrophobic of a polymer is. Results of water absorption of polymers are demonstrated in Table 5. Non-fluorinated polymer PEMA has the highest water absorption value among four polymers, so PEMA is the least hydrophobic. As expected, PDFHMA is the most hydrophobic because its water absorption value is the lowest one. Thus, the hydrophobicity results from water absorption are well consistent with that measured by contact angles and surface energy.

Conclusion

Three fluorinated copolymers were prepared in "one pot" using a surface-active ATRP initiator under AGET ATRP in emulsion conditions. The surface-active ATRP initiator and OP-10 can form a synergistic stabilizing system that guarantees the stability of final latex. Kinetic studies of the emulsion polymerization of

PTFEMA-*b*-PS demonstrate that the polymerization has living/controlled characteristics. The fluorinated copolymers have low-surface energy with hydrophobic performance, compared with non-fluorinated polymers such as PS. The PDFHMA-*b*-PS copolymer that has a relatively long-chain-unit reveals the lowest surface energy among the three fluorinated copolymers, which has promising applications as low-surface energy materials and coatings. The water-based living emulsion polymerization method for preparing fluorinated block copolymers is of great significance both in academics and industry due to its convenience and environmental friendliness.

Chemical structures of organic compounds and polymers in Fig. 1, Scheme 1, and Fig. 8 are drawn by ChemDraw Ultra 8.0 soft ware. ^{1}H NMR spectrum of Fig. 8 is from MestReC NMR program. Figure 2 is a photo of real latex samples created by a digital camera. Figures 4, 5, and 6 are formed by Origin 7.5 program.

Acknowledgments This work was financially supported by the Natural Science Foundations of China (No. 51063002 and No. 50503009) and the Natural Science Foundations of Jiangxi Province (No. 2009GZH0035).

References

1. Gao HF, Matyjaszewski K (2009) Synthesis of functional polymers with controlled architecture by CRP of monomers in the presence of cross-linkers: from stars to gels. Prog Polym Sci 34:317–350
2. Sciannamea V, Jrme R, Detrembleur C (2008) In situ nitroxide-mediated radical polymerization (NMP) processes: their understanding and optimization. Chem Rev 108:1104–1126
3. Ouchi M, Terashima T, Sawamoto M (2008) Precision control of radical polymerization via transition metal catalysis: from dormant species to designed catalysts for precision functional polymers. Acc Chem Res 41:1120–1132
4. Dasgupta A, Klapper M, Müllen K (2008) Controlled polymerization of N-trimethylsilyl methacrylamide: a new polymethacrylamide precursor. Polym Bull 60:199–210
5. Zhang LF, Cheng ZP, Zhou NC, Shi SP, Su XR, Zhu XL (2009) Synthesis of miktoarm dumbbell-like amphiphilic triblock copolymer by combination of consecutive RAFT polymerizations and ATRP. Polym Bull 62:11–22
6. Gordin C, Delaite C, Medlej H, Josien-Lefebvre D, Hariri K, Rusu M (2009) Synthesis of ABC miktoarm star block copolymers from a new heterotrifunctional initiator by combination of ATRP and ROP. Polym Bull 63:789–801
7. Zhang LF, Cheng ZP, Zhang ZB, Xu DY, Zhu XL (2010) Fe(III)-catalyzed AGET ATRP of styrene using triphenyl phosphine as ligand. Polym Bull 64:233–244
8. Patten TE, Xia J, Abernathy T, Matyjaszewski K (1996) Polymers with very low polydispersities from atom transfer radical polymerization. Science 272:866–868
9. Tsarevsky NV, Matyjaszewski K (2007) ''Green'' atom transfer radical polymerization: from process design to preparation of well-defined environmentally friendly polymeric materials. Chem Rev 107:2270–2299
10. Zhang WD, Zhang W, Zhang ZB, Zhu J, Pan QM, Zhu XL (2009) Synthesis and characterization of AB2-type star polymers via combination of ATRP and click chemistry. Polym Bull 63:467–483
11. Zhao K, Cheng ZP, Zhang ZB, Zhu J, Zhu XL (2009) Synthesis of fluorescent poly(methyl methacrylate) via AGET ATRP. Polym Bull 63:355–364
12. Shen L, Ma C, Pu SZ, Cheng CJ, Xu JK, Li L, Fu CQ (2009) Synthesis and properties of novel photochromic poly(methyl methacrylate-co-diarylethene)s. New J Chem 33:825–830
13. Wan WM, Pan CY (2008) A facile strategy to control polymer topology by variation of controlled radical polymerization mechanisms. Chem Commun 5639–5641
14. Lu XJ, Gong SL, Meng LZ, Li C, Liang F, Wu ZQ, Zhang LF (2007) Novel fluorescent amphiphilic block copolymers: controllable morphologies and size by self-assembly. Eur Polym J 43:2891–2900

15. Xia JH, Johnson T, Gaynor SG, Matyjaszewski K, DeSimone JM (1999) Atom transfer radical polymerization in supercritical carbon dioxide. Macromolecules 32:4802–4805
16. Lu JM, Yan F, Texterc J (2009) Advanced applications of ionic liquids in polymer science. Prog Polym Sci 34:431–448
17. Hu ZQ, Shen XR, Qiu HY, Lai GQ, Wu JR, Li WQ (2009) AGET ATRP of methyl methacrylate with poly(ethylene glycol) (PEG) as solvent and TMEDA as both ligand and reducing agent. Eur Polym J 45:2313–2318
18. Sheldon RA (2005) Green solvents for sustainable organic synthesis: state of the art. Green Chem 7:267–278
19. Cunningham MF (2008) Controlled/living radical polymerization in aqueous dispersed systems. Prog Polym Sci 33:365–398
20. Save M, Guillaneuf Y, Gilbert RG (2006) Controlled radical polymerization in aqueous dispersed media. Aust J Chem 59:693–711
21. Cheng CJ, Gong SS, Fu QL, Shen L, Liu ZB, Qiao YL, Fu CQ (2010) Hexamethylenetetramine as both a ligand and a reducing agent in AGET atom transfer radical batch emulsion polymerization. Polym Bull. doi:10.1007/s00289-010-0305-y
22. Oh JK (2008) Recent advances in controlled/living radical polymerization in emulsion and dispersion. J Polym Sci A 46:6983–7001
23. Xu LQ, Yao F, Fu GD, Shen L (2009) Simultaneous ''click chemistry'' and atom transfer radical emulsion polymerization and prepared well-defined cross-linked nanoparticles. Macromolecules 42:6385–6392
24. Cheng CJ, Shu JB, Gong SS, Shen L, Qiao YL, Fu CQ (2010) Synthesis and use of a surface-active initiator in emulsion polymerization under AGET and ARGET ATRP conditions. New J Chem 34:163–170
25. Cheng XJ, Zhao Q, Yang YK, Tjong SC, Li RKY (2010) A facile method for the synthesis of ZnS/polystyrene composite particles and ZnS hollow micro-spheres. J Mater Sci 45:777–782
26. Li WW, Min K, Matyjaszewski K, Stoffelbach F, Charleux B (2008) PEO-based block copolymers and homopolymers as reactive surfactants for AGET ATRP of butyl acrylate in miniemulsion. Macromolecules 41:6387–6392
27. Stoffelbach F, Griffete N, Buiab C, Charleux B (2008) Use of a simple surface-active initiator in controlled/living free-radical miniemulsion polymerization under AGET and ARGET ATRP conditions. Chem Commun 4807–4809
28. Rieger J, Osterwinter G, Bui C, Stoffelbach F, Charleux B (2009) Surfactant-free controlled/living radical emulsion (co)polymerization of *n*-butyl acrylate and methyl methacrylate via RAFT using amphiphilic poly(ethylene oxide)-based trithiocarbonate chain transfer agents. Macromolecules 42:5518–5525
29. Wang XG, Luo YW, Li BG, Zhu SP (2009) Ab initio batch emulsion RAFT polymerization of styrene mediated by poly(acrylic acid-*b*-styrene) trithiocarbonate. Macromolecules 42:6414–6421
30. Ji J, Yan LF, Xie DH (2008) Surfactant-free synthesis of amphiphilic diblock copolymer in aqueous phase by a self-stability process. J Polym Sci A 46:3098–3107
31. Jakubowski W, Matyjaszewski K (2005) Activator generated by electron transfer for atom transfer radical polymerization. Macromolecules 38:4139–4146
32. Jakubowski W, Min K, Matyjaszewski K (2006) Activators regenerated by electron transfer for atom transfer radical polymerization of styrene. Macromolecules 39:39–45
33. Jakubowski W, Matyjaszewski K (2006) Activators regenerated by electron transfer for atom-transfer radical polymerization of (meth)acrylates and related block copolymers. Angew Chem Int Ed 45:4482–4486
34. Reisinger JJ, Hillmyer MA (2002) Synthesis of fluorinated polymers by chemical modification. Prog Polym Sci 27:971–1005
35. Aminuzzaman M, Mitsuishi M, Miyashita T (2010) Fabrication of fluorinated polymer nanosheets using the Langmuir–Blodgett technique: characterization of their surface properties and applications. Polym Int 59:583–596
36. Nenov S, Hoffmann MS, Steffen W, Klapper M, Müllen K (2009) Fluorous miniemulsions: a powerful tool to control morphology in metallocene-catalyzed propene polymerization. J Polym Sci A 47:1724–1730
37. Nenov S, Clark CG, Klapper M, Müllen K (2007) Metallocene-catalyzed polymerization in non-aqueous fluorous emulsion. Macromol Chem Phys 208:1362–1369

38. Tavana H, Gitiafroz R, Hair ML, Neumann AW (2004) Determination of solid surface tension from contact angles: the role of shape and size of liquid molecules. J Adhesion 80:705–725
39. Park IJ, Lee S, Choi CK, Kim K (1996) Surface properties and structure of poly (perfluoroalkylethyl methacrylate). J Colloid Interface Sci 181:284–288
40. Min K, Gao HF, Matyjaszewski K (2005) Preparation of homopolymers and block copolymers in miniemulsion by ATRP using activators generated by electron transfer (AGET). J Am Chem Soc 127:3825–3830
41. Ibrahim KA, Al-Muhtaseba AH, Seppal J (2009) Synthesis of poly(fluorinated styrene)-*block*-poly(ethylene oxide) amphiphilic copolymers via atom transfer radical polymerization: potential application as paper coating materials. Polym Int 58:927–932
42. Chen L, Zhao YR, Deng M, Yuan DX, Ni HG, Zhang W, Wang XP (2010) Surface properties and chain structure of fluorinated acrylate copolymers prepared by emulsion polymerization. Polym Bull 64:81–97